

SINERGI Vol. 29, No. 3, October 2025: 563-572 http://publikasi.mercubuana.ac.id/index.php/sinergi http://doi.org/10.22441/sinergi.2025.3.001



Heat transfer and pressure characteristics of Tri Ethylene Glycol/water and Ethylene Glycol/water mixtures in copper pipe heated flow systems



Sukarman^{1,2*}, Khoirudin^{1,2}, Amir¹, Nazar Fazrin¹, Renata Lintang Azizah³, Muji Setiyo^{4,5}, W. H. Azmi⁶

¹Department of Mechanical Engineering, Faculty of Engineering, Universitas Buana Perjuangan Karawang, Indonesia ²Centre of Research and Innovation in Energy Conversion and Nanoparticle Technology, Universitas Buana Perjuangan Karawang, Indonesia.

³Department of Mechanical Engineering Education, Faculty of Technology and Vocational Education, Universitas Pendidikan Indonesia, Indonesia.

⁴Department of Sustainable Engineering, Saveetha School of Engineering, Saveetha Medical and Technical Science, India. ⁵Department of Mechanical Engineering, Faculty of Automotive Engineering, Universitas Muhammadiyah Magelang, Indonesia ⁶Centre for Research in Advanced Fluid and Processes, Universiti Malaysia Pahang Al-Sultan Abdullah, Malaysia

Abstract

Enhancing heat transfer efficiency and pressure regulation in copper pipe flow systems is crucial for advancing modern cooling and heating technologies, particularly given the widespread use of copper piping in these applications. This study investigates the thermal and hydraulic performance of ethylene glycol/water (EG/water) and tri ethylene glycol/water (TEG/water) mixtures as working fluids in copper pipe systems. A series of controlled experiments was carried out on a dedicated copper pipe test section to evaluate the effects of varying flow rates on the heat transfer coefficient and pressure drop for each fluid mixture. The results indicate that the TEG/water mixture yielded a ~2.0% increase in heat transfer coefficient and a ~1.0% reduction in pressure drop compared to the EG/water mixture, with a corresponding increase in Reynolds number of approximately 37.0%. The reduction in pressure drop is primarily attributed to the lower viscosity of the TEG/water fluid. These findings provide valuable comparative insights into the thermophysical behaviour of both glycolbased mixtures and offer practical guidance for optimizing the selection of thermal fluids in large-scale cooling and heating systems that utilize copper piping.

This is an open-access article under the CC BY-SA license.



Keywords:

Copper Pipe Heated; Ethylene Glycol; Heat transfer coefficient; Pressure drops; Tri ethylene Glycol/Water;

Article History:

Received: December 16. 2023 Revised: February 19, 2024 Accepted: March 20, 2024 Published: September 1, 2025

Corresponding Author:

Sukarman
Department of Mechanical
Engineering, Universitas Buana
Perjuangan Karawang,
Indonesia
Email:

sukarman@ubpkarawang.ac.id

INTRODUCTION

Improving the heat transfer efficiency and managing the pressure characteristics of copper pipe flow systems are essential for advancing thermal management in modern heating and cooling technologies. Copper pipes have been widely adopted in various systems because of their high durability, thermal conductivity, and flexibility. However, although water is traditionally used as a working fluid, it exhibits rapid evaporation due to its relatively low boiling point, making it unsuitable for high-temperature applications.

The structural design of thermal systems, as well as the nature of the working fluid, significantly influence the system's efficiency. Utilizing high-boiling-point fluids in thermal systems enhances performance and supports efforts to achieve the Sustainable Development Goals (SDGs), particularly in the areas of clean water access and sanitation. Fluids such as ethylene glycol (EG) and tri ethylene glycol (TEG) are increasingly utilized because of their high boiling points and stability under thermal loads [1, 2, 3]. Although EG is more commonly integrated into HVAC and industrial thermal

applications, despite being chemically similar, TEG has more limited use owing to its higher viscosity and cost.

The heat transfer coefficient is a crucial quantitative measure for evaluating the rate at which heat is conducted from a fluid to a surface [4][5]. It reflects the fluid's capacity to conduct heat and is influenced by the physical properties of the fluid, flow velocity, surface properties, and thermophysical conditions [6, 7, 8, 9, 10]. The key parameters affecting the HTC include fluid density [11][12], velocity [13, 14, 15], thermal conductivity [16][17], viscosity [18], and the addition of nanoparticles to the base fluid [19]. Accurate HTC characterization is essential for designing and optimizing thermal systems, such as heat exchangers [19][20] and advanced cooling systems, which directly affect their heat transfer performance and energy efficiency [21][22].

Heat transfer units are vital components in industrial and residential settings, including power generation units, automotive systems, and climate control infrastructure [23, 24, 25]. Optimizing these systems requires balancing the performance with the hydraulic efficiency to achieve high heat transfer rates while minimizing pressure loss [26, 27, 28]. Although pressure drop and heat transfer are interdependent, they are frequently analyzed in isolation. This disconnection may hinder the holistic optimization of systems. EG- and TEGbased fluids are widely used in industrial thermal management, vehicle cooling systems, and HVAC units [29], and their effectiveness is significantly influenced by their mixing ratios with water [30]. The selection of EG/water or TEG/water compositions is typically dictated by operational requirements such as freezing point depression and target working temperature ranges.

Numerous studies have examined the performance of glycol-based water mixtures [31].

Manik et al. [32] investigated a 40:60 EG/water mixture functioning as the cold-side fluid, while hot water was the heat source. They evaluated the thermal performance using a radiator with varying hot-fluid discharge rates ranging from 6.7 to 27 LPM. In a separate investigation, Abolarin et al. [33] analyzed the pressure drop and heat transfer using twisted tape inserts across test sections under varying flow regimes. Their setup, as shown in Figure 1, operated with a constant heat flux between 1.35 and 4 kW/m², covering Reynolds numbers ranging from 300 to 11,404, including laminar, transitional, and turbulent flows.

Ghozatloo et al. [34] examined EG-based nanofluids with graphene (Grn) at concentrations of 0.1–1.5% using a shell-and-tube heat exchanger (STHE), where the EG/Grn nanofluid circulated on the cold side and pure EG on the hot side of the STHE. The heat convection efficacy was compared with that of the EG systems. Azari et al. [35] investigated the local and overall heat transfer coefficients using a 40:60 EG/water mixture, offering insights into heat exchanger applications.

This study investigated the thermal performance of EG/water and TEG/water mixtures in a heated copper pipe system. This study examined the interdependence between HTC. fluid flow rate, and pressure drop, providing a foundational understanding of these glycol-based fluids under varying conditions. Although studies have explored similar working fluids, comprehensive analyses of the HTC and friction factor (Fr) correlation within single-pipe configurations, particularly for EG/water and TEG/water at 60 °C and a 40:60 volume ratio, remain limited. This study addresses this gap through systematic experiments conducted across various flow rates to determine the volumetric relationships that affect thermal and hydraulic responses.

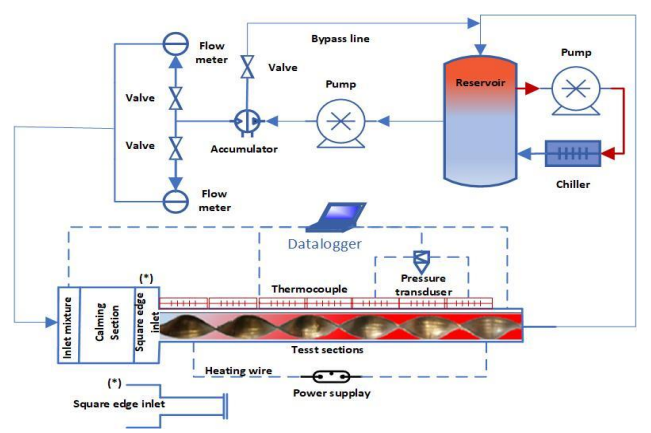


Figure 1. Experimental test section and configuration (adapted from [33])

The results aim to provide insights for optimizing thermal systems using glycol-water mixtures, while establishing a baseline for future studies involving additive integration, to enhance heat transfer efficiency in systems transitioning from moderate to high-performance regimes.

METHOD Properties of Ethylene Glycol and Tri Ethylene Glycol

The thermophysical properties of fluid mixtures are fundamental to heat transfer applications in industrial and engineering systems [36]. EG has a melting point of -13 °C and a boiling point of 197.3 °C, respectively. At 20 °C, EG exhibits favorable heat transfer behavior with a specific heat capacity of approximately 2430 J/kg·K, thermal conductivity of 0.25 W/m·K, and density of 1113.4 kg/m³ [30]. Water exhibits excellent thermal storage characteristics at this temperature, with a specific heat capacity of 4180 J/kg K and a density of 998.2 kg/m³. Its thermal conductivity of 0.606 W/m·K enhances its functionality as a heat-transfer medium. A comprehensive understanding of these thermophysical parameters is essential for designing or optimizing systems involving TEG/water and EG/water mixtures for cooling. and industrial fluid circulation applications. Table 1 lists the representative thermophysical properties of the TEG used in this study.

Experimental Configuration

The experimental setup consisted of a copper test section with an inner diameter of 18

mm and a wall thickness of 1.5 mm. Ten K-type thermocouples (T_1 – T_{10}) were mounted along the pipe wall, with additional sensors at the inlet (T_i) and outlet (T_o) to monitor the fluid temperatures. Pressure sensors were placed at both ends (P_i and P_o), and a centrifugal pump circulated the working fluid from a 20 L reservoir. All the sensors were calibrated before testing to ensure measurement accuracy.

Heating was supplied by two 1500 W tubular heaters, regulated by a variable voltage controller (220 VAC, 50/60 Hz, up to 250 VAC). The temperature, pressure, and flow rate were recorded at one-second intervals using a calibrated data logger with accuracies of ±0.1°C, ±0.1 psi, and ±0.01 L/min, respectively. The tests commenced when the inlet temperature reached 60 °C and were stabilized using a chiller acting as heat exchanger. All experiments were controlled conducted under environmental conditions to ensure the repeatability of the results. A schematic of the test loop is presented in Figure 2.

Heat transfer coefficient (HTC), h

The HTC characterizes the thermal energy transfer between the surface and the surrounding fluid. Its magnitude depends on the fluid velocity, geometric configuration, temperature gradient, and thermal properties of the materials involved. HTC is crucial in evaluating heat exchange mechanisms, particularly in convection processes and phase transitions involving liquid–solid interactions.

Table 1	Thermonhysical	properties of the	TFG/water	mixture with	a volume ratio	of 40:60 [37][38]
I able I.	HIIGHHUUHIVSICAI		, ILG/Water	IIIIXLUIG WILII	a volullic lallo	01 40.00 137 11301

Temperature (K)	Density (kg/m³)	Viscosity (Pa.s)	Heat Specific (J/kg. K)	Thermal conductivity (W/m. K)
273	273	0.0110	3457	0.416
278	278	0.0084	3487	0.417
283	283	0.0070	3517	0.417
288	288	0.0059	3546	0.418
293	293	0.0051	3575	0.418
298	298	0.0043	3603	0.418
303	303	0.0037	3631	0.419
313	308	0.0032	3657	0.420
323	313	0.0028	3683	0.420
333	318	0.0024	3708	0.420
343	323	0.0021	3733	0.421
353	328	0.0019	3757	0.422
363	333	0.0016	3781	0.422
373	338	0.0015	3803	0.422
393	343	0.0013	3825	0.423
413	348	0.0012	3847	0.424
433	353	0.0010	3869	0.424
453	358	0.0009	3888	0.424
473	363	0.0008	3907	0.425

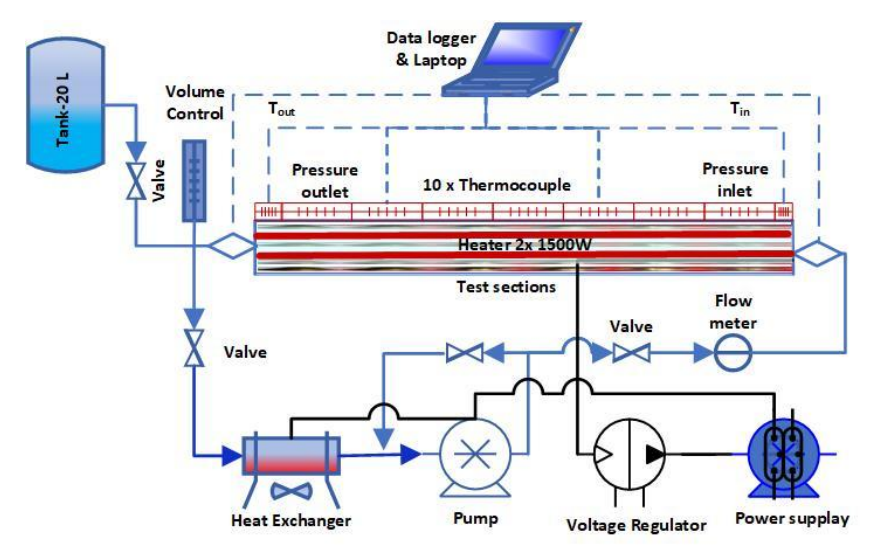


Figure 2. Experimental setup

The convective heat transfer coefficient, h, was obtained from (1) [39]:

$$h = \frac{Q}{Ts - Tm} \tag{1}$$

where T_s denotes the average surface temperature (K) at the suction test location, calculated using (2) [25].

$$T_{s} = \frac{(\sum_{i=1}^{8} T)}{10}$$
 where T_{m} is the bulk fluid temperature, which is

calculated using (3):

$$T_m = \frac{T_{in} - T_{out}}{2} \tag{3}$$

In this study, the heat transfer rate, Q (W), was evaluated as the average of the power input and the fluid-based heat transfer, as expressed in (4) [32]:

$$Q = \frac{Q_1 + Q_2}{2} \tag{4}$$

where Q₁ denotes the heat transfer rate (W) from the power input, calculated using Eq. (5), and Q_2 reflects the fluid-based heat transfer rate from (6) [40].

$$Q_1 = VI \tag{5}$$

$$Q_1 = VI$$

$$Q_2 = \dot{m}C_p(T_o - T_i)$$
(5)
(6)

where V, I, C_p , and \dot{m} represent the voltage (V), current (A), specific heat capacity (J/kg·K), and mass flow rate (kg/s), respectively. The heat flux, in W/m², quantifies the thermal energy transferred per unit area.

The heat flux (q'') was computed using Eq. (7), with heat input (Q) derived from voltage, current, mass flow rate, and fluid specific heat [32]. Here, D and L denote the pipe's inner diameter (m) and length (m).

$$q^{\prime\prime} = \frac{Q}{\pi D I} \tag{7}$$

Hydrodynamic and Thermal Characterization

Reynolds number (Re) is a dimensionless parameter that represents the ratio of inertial to viscous forces within a fluid flow, serving as a fundamental criterion distinguishing between laminar, transitional, and turbulent flow regimes. It is defined by (8) [41, 42, 43].

$$Re = \frac{\rho vD}{\mu} \tag{8}$$

where ρ is fluid density (kg/m³), ν is velocity (m/s), D is hydraulic diameter (m), and μ is dynamic viscosity (mPa·s)

Nusselt The number (*Nu*) dimensionless parameter that characterizes the enhancement of heat transfer owing to convection relative to pure conduction across a thermal boundary layer. It is defined in (9) [44][45].

$$Nu = \frac{hD}{k} \tag{9}$$

This study estimated the Nusselt number (Nu) using two well-established empirical correlations: the Dittus-Boelter equation and the Notter-Rouse correlation, as expressed in (10) and (11) [46].

$$Nu = 0.023Re^{0.8}Pr^{0.4} (10)$$

$$Nu = 5 + 0.015Re^{0.856}Pr^{0.347} \tag{11}$$

Pressure Drops and Friction Factor

The pressure drops (ΔP) , expressed in pascals (Pa), reflect the energy losses owing to friction. flow separation, and geometrical variations along the flow path. This parameter is key to assessing flow efficiency and system performance. The friction factor dimensionless quantity, characterizes the wall shear-induced resistance and depends on the flow

regime, surface roughness, and channel geometry. In this study, ΔP was measured between the inlet and outlet of the test section, and the friction factor was used to evaluate the hydraulic performance. The pressure drop was calculated using (12) [39]:

$$\Delta P = P_{in} - P_{out} \tag{12}$$

The Darcy friction factor (f) is a dimensionless parameter essential for quantifying frictional losses in internal flows and is critical for predicting pressure drops in piping systems. This dimensionless parameter was calculated experimentally using (13), which relates the pressure drop (Δ P), pipe length (L), hydraulic diameter (D), fluid density (ρ), and mean velocity (ν) [47].

$$f = \frac{\Delta P}{\left(\frac{L}{D}\right)\left(\rho_f \frac{v^2}{2}\right)} \tag{13}$$

In addition to experimental measurements, *f* can be estimated using empirical correlations. For turbulent flow in smooth tubes, the Petukhov correlation is expressed in (14) [35]:

$$f = (0.79 \ln Re - 1.64)^{-2} \tag{14}$$

For lower Reynolds numbers or transitional regimes, the Blasius correlation provides an empirical estimate of the Darcy friction factor, as expressed in (15) [35]:

$$f = \frac{0.3164}{Re^{0.25}} \tag{15}$$

These formulations are used in thermal-fluid system design to evaluate energy losses from the wall shear stress and flow resistance.

RESULTS AND DISCUSSION Analysis of Heat Transfer Coefficient (HTC), h

HTC was determined using (1). Experimental observations were used to assess the effect of varying flow rates on EG/water and

TEG/water mixtures. The results showed a direct relationship between the Reynolds number (Re) and HTC, confirming that a higher flow velocity promotes convective heat transfer. A marked enhancement in HTC occurred as the flow rate increased from 4 LPM to above 12 LPM, indicating improved thermal performance under higher turbulence. This behavior aligns with classical heat transfer principles, wherein higher flow rates lead to thinner thermal boundary layers and more efficient heat transfer. Based on these findings, new empirical correlations for estimating the HTC in TEG/water and EG/water mixtures were formulated in (16) and (17).

$$h_{TEG/Water} = 160.1 + 84.24 flowrate$$
 (16)

$$h_{EG/Water} = 163.1 + 82.32 flowrate$$
 (17)

The findings of this study reaffirm the theoretical understanding that the heat transfer rate increases proportionally with the HTC, which is consistent with previous reports [32]. Furthermore, a strong positive correlation between heat transfer and fluid flow rates, as extensively documented in the literature [29], was substantiated. experimental data also revealed a direct relationship between the mass and volumetric flow rates of the working fluid, corroborating the results of previous studies [34][48]. As shown in Figure 3, higher fluid flow rates led to enhanced HTC values, which were attributed to more vigorous convective transport phenomena. The fluid flow rate directly influences the Reynolds number (Re), with higher flow rates resulting in higher Re. To further clarify this relationship, an analysis was conducted to examine the impact of Re on the HTC. The results indicate that the HTC reached its maximum at Re values exceeding 5500 for the TEG/water mixture and 9000 for the EG/water mixture.

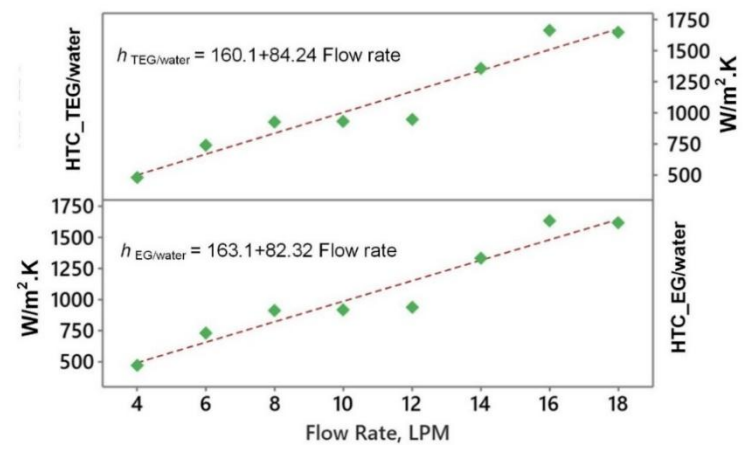


Figure 3. Impact of EG/water flow rate on the heat transfer coefficient

Conversely, the lowest HTC values were observed at Re values of approximately 2000, as shown in (18) and (19).

$$HTC_{TEG/Water} = 81.9 + 0.2893Re$$
 (18)

$$HTC_{EG/Water} = 81.3 + 0.2793$$
Re (19)

These findings demonstrate a significant increase in HTC as a function of Re, with both base fluids exhibiting a linear trend, as shown in Figure 4 (a). A similar linear behavior was observed concerning the pressure drop (ΔP), where an increase in ΔP corresponded to higher HTC values (Figure 4b). This correlation is expressed by. (20) and (21):

$$HTC_{TEG/Water} = 416.7 + 0.4228 \,\Delta P$$
 (20)

$$HTC_{EG/Water} = 414.3 + 0.4092 \Delta P$$
 (21)

These linear correlations suggest that the enhancement in convective heat transfer is strongly associated with increased flow velocity and the pressure drop. Fluid dynamics principles support the underlying physical mechanisms and can be further understood by interpreting the fundamental formulations in (1), (8), (9), (10), and (11) [39, 41, 43, 45, 46]. The overall influence of the Re variation on the HTC is illustrated in Figure 4

Pressure drops, friction factor, and Reynolds number analysis

The pressure drop (ΔP) and Darcy friction factor (f) were calculated using (12). The average pressure drop values were subsequently analyzed to assess the effect of the Reynolds number (Re) on the flow behavior of the EG/water mixture. Figure 5 shows a consistent increase in ΔP with increasing Re, indicating a direct relationship flow velocity and hydraulic between the resistance. The lowest Re values corresponded to a pressure drop of approximately 500 Pa. In contrast, the highest Re values were associated with a ΔP of approximately 5500 Pa for the TEG/water mixture and 9000 Pa for the MEG/water mixture. Based on Bernoulli's principle (8), Re is strongly influenced by the flow velocity,

which is directly proportional to the pressure difference, as indicated in (22) [49].

$$\Delta P = P_1 - P_2 = \left(\frac{\rho v_2^2}{2} + \rho g h_2\right) - \left(\frac{\rho v_1^2}{2} + \rho g h_1\right)$$
 (22)

Given h1 = h2, (22) can be rewritten as follows:

$$\Delta P = P_1 - P_2 = \left(\frac{\rho v_2^2}{2}\right) - \left(\frac{\rho v_1^2}{2}\right)$$
 (23)

The Darcy friction factor was determined experimentally using (13) and compared with the theoretical values calculated from Petukhov and Blasius correlations (14) and (15), respectively [33]. As illustrated in Figure 6, the friction factor decreased with increasing Reynolds number for both the TEG/water and EG/water mixtures at all temperatures. This inverse relationship closely followed the trends predicted by the Petukhov and Blasius models, confirming the consistency between the experimental and theoretical results. The highest friction factor values occurred near Re ≈ 2000, indicating the onset of the laminar-to-turbulent flow transition at this Reynolds number.

Conversely, the lowest friction factors were observed in the fully turbulent regime, specifically at Re > 5500 for TEG/water and Re > 9000 for EG/water, respectively. This trend reflects the decreasing flow resistance as inertial forces increasingly dominate viscous forces, which aligns with the expected behavior during the laminar-toturbulent transition in thermal-fluid systems. These findings are consistent with previous reports [34][35], which highlight the inverse relationship between the friction factor and Reynolds number (Re) and the associated impact on the pressure drop. In this study, the fluid velocity and flow rate increased proportionally with Re, reinforcing the established understanding that Re is primarily governed by the flow rate and fluid properties [30][29]. Consequently, the friction factor decreased as Re increased, accompanied by reduced pressure drops at higher flow rates, an outcome that aligns with Bernoulli's principle and well-established hydrodynamic models.

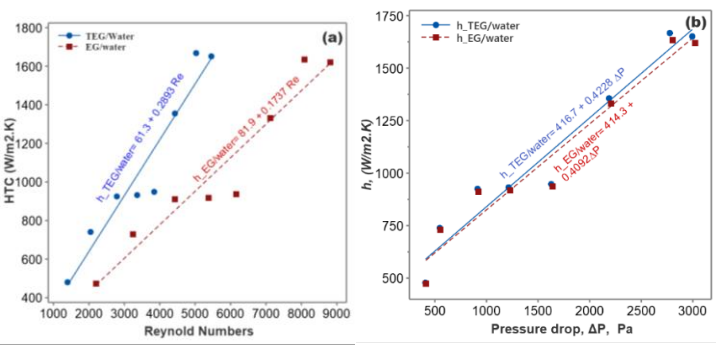


Figure 4. The effect of the EG/Water fluid flow rate on the Nusselt number

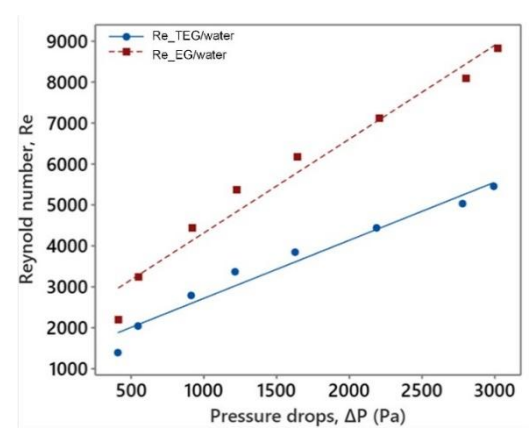


Figure 5. Effect of Reynolds number on pressure drop

Analysis of Reynolds number (Re) and Flow rate correlations

The Nusselt number (Nu) was evaluated against the predictions from the Dittus-Boelter (10) and Notter-Rouse (11) correlations, considering the variations in the flow rate. As shown in Figure 7, Nu increased consistently with the flow rate, ranging from a minimum of 4 LPM to a maximum of 18 LPM. The experimental data showed strong agreement with the Dittus-Boelter predictions at moderate and high flow rates, whereas the Notter-Rouse model tended to

underestimate Nu under similar conditions.

This behavior supports the theoretical correlation between Nu, Re, and HTC, as outlined in (9) and discussed in [25, 32, 33]. Because the flow rate and fluid properties directly influence Re, the observed increase in Nu at higher flow rates confirms their interdependency. These results are consistent with previous findings [29], which identified the flow rate as the dominant factor influencina the convective heat transfer performance. In this study, Nu exhibited a clear positive correlation with the fluid flow rate [50]. An increase in the flow rate consistently resulted in higher Nu values, indicating the fluid medium's enhanced convective heat transfer performance. This behavior is consistent with the theoretical expectation that a higher velocity promotes thinner thermal boundary layers, thereby improving heat transfer efficiency.

Figure 7(b) illustrates the relationship between flow rate and pressure drop. The data indicate that the pressure drop increased proportionally with the flow rate. This trend is well explained by Bernoulli's principle and energy conservation across the flow domain, as described by (16) and (17) [49], which underscores the trade-off between the thermal enhancement and hydrodynamic penalties in forced convection systems.

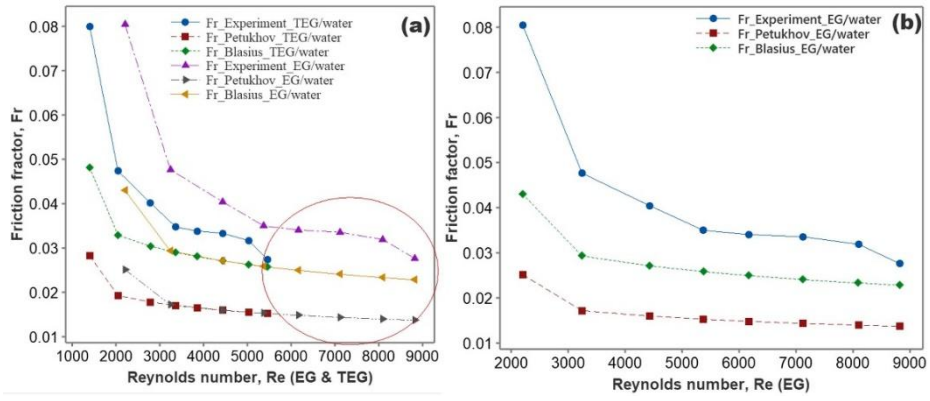


Figure 6. Effect of Reynolds number on friction factor: (a) TEG/water and EG/water, (b) EG/water.

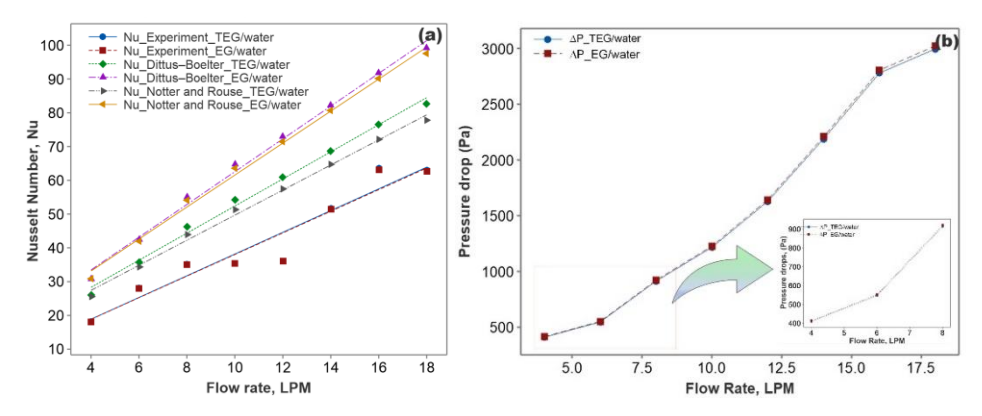


Figure 7. Effect of flow rate on (a) Nusselt number and (b) pressure drop

CONCLUSION

This study investigated the heat transfer coefficient (HTC) and pressure drop (ΔP) in copper pipe flow systems using TEG/water and EG/water binary fluids at a 40:60 volumetric ratio and an operating temperature of 60 °C. The results demonstrate that variations in the flow rate significantly influence both the HTC and ΔP , highlighting the interplay between the thermal performance and hydrodynamic resistance in such binary coolant systems.

- a. The rising heat transfer coefficient (HTC) observed in both the TEG/water and EG/water fluids passing through the copper pipe, in conjunction with increased flow rates, can be attributed to the corresponding increase in the Reynolds number, directly proportional to the higher flow rates. Consequently, the TEG/water fluid had a higher HTC than the EG/water fluid.
- b. The ΔP within the fluid in the copper pipe directly increased with the flow rate, whereas the friction factor in the TEG/water and EG/water fluids decreased as the flow rate increased.
- **c.** The Reynolds number of the fluid within the copper pipe maintained a directly proportional relationship with the fluid flow rate throughout the study.

ACKNOWLEDGMENT

We thank the Ministry of Research, Technology, & Higher Education for fully funding this research through the "Penelitian Dosen Pemula" program with numbers 053/SPH2H/RT-MONO/LL42023 and 02/LPPM/PDP/VII/2023. The authors sincerely thank the dedicated team at Buana Perjuangan University's Energy Conversion Laboratory in Karawang for their invaluable assistance with data collection during the experimental process.

REFERENCES

- [1] M. A. Khattak, Mukhtar A, and S. Kamran Afalaq, "Application of nanofluids in heat exchangers: A review," *Journal of Advanced Research in Materials Science*, vol. 66, no. 1, pp. 5625-5638, 2020, doi: 10.37934/arms.66.1.818.
- [2] A. I. Ramadhan et al., "Experimental and numerical study of heat transfer and friction factor of plain tube with hybrid nanofluids," Case Studies in Thermal Engineering, vol. 22, p. 100782, 2020, doi: 10.1016/j.csite.2020. 100782.
- [3] M. A. B. Sidik et al., "Development of insulation oil based on Palm Oil Mill Effluent

- with nano silica," *Sinergi,* vol. 28, no. 2, 2024, doi: 10.22441/sinergi.2024.2.018.
- [4] M. S. Liu et al., "Enhancement of Thermal Conductivity with CuO for Nanofluids," Chemical Engineering & Technology, vol. 29, no. 1, pp. 72-77, 2006, doi: 10.1002/ceat.200500184.
- [5] M. Y. Hanna et al., "Application of the detailed balance model to thermoradiative cells based on a p-type two-dimensional indium selenide semiconductor," *Sinergi*, vol. 26, no. 1, 2022, doi: 10.22441/sinergi.2022.1.015.
- [6] M. Mehrpooya et al., "Heat transfer and economic analyses of using various nanofluids in shell and tube heat exchangers for the cogeneration and solar-driven organic Rankine cycle systems," *International Journal of Low-Carbon Technologies*, vol. 17, no. November, pp. 11-22, 2022, doi: 10.1093/ijlct/ctab075.
- [7] E. Borri et al., "Phase Change Slurries for Cooling and Storage: An Overview of Research Trends and Gaps," *Energies*, vol. 15, no. 19, 2022, doi: 10.3390/en15196873.
- [8] R. LeSar, "Materials selection and design," *Introduction to Computational Materials Science*, pp. 269-278, 2013, doi: 10.1017/cbo9781139033398.015.
- [9] H. Ibrahim e tal., , "A review on factors affecting heat transfer efficiency of nanofluids for application in plate heat exchanger," *Journal of Advanced Research in Fluid Mechanics and Thermal Sciences*, vol. 60, no. 1, pp. 144-154, 2019.
- [10] A. Ghozatloo, A. Rashidi, and M. Shariaty-Niassar, "Convective heat transfer enhancement of graphene nanofluids in shell and tube heat exchanger," *Experimental Thermal and Fluid Science*, vol. 3, pp. 136-141, 2014, doi: 10.1016/j.expthermflusci. 2013.11.018.
- [11] W. Zheng et al., "Numerical and experimental investigation of a helical coil heat exchanger for seawater-source heat pump in cold region," *International Journal of Heat and Mass Transfer*, vol. 96, pp. 1-10, 2016, doi: 10.1016/j.ijheatmasstransfer. 2016.01.022.
- [12] Sukarman et al., "Multi-technique characterization of TiO2 nanoparticles: Crystallite size, microstrain, and phase analysis for nanomaterial applications a review," *Hybrid Advances*, vol. 11, 2025, doi: 10.1016/j.hybadv.2025.100523.
- [13] M. Bayareh et al., "Numerical study of the effects of stator boundary conditions and blade geometry on the efficiency of a scraped surface heat exchanger," *Applied Thermal*

- Engineering, vol. 113, pp. 1426-1436, 2017, doi: 10.1016/j.applthermaleng.2016.11.166.
- [14] B. C. Pak and Y. I. Cho, "Hydrodynamic and Heat Transfer Study of Dispersed Fluids With Submicron Metallic Oxide," *Experimental Heat Transfer: A Journal of, Thermal Energy Transport, Storage, and Conversion,* vol. 11, no. 2, pp. 151-170, 2007, doi: 10.1080/08916159808946559.
- [15] L. Godson et al., "Heat transfer characteristics of silver/water nanofluids in a shell and tube heat exchanger," *Archives of Civil and Mechanical Engineering*, vol. 14, no. 3, pp. 489-496, 2014, doi: 10.1016/j.acme.2013.08.002.
- [16] Z. Said et al., "Heat transfer enhancement and life cycle analysis of a Shell-and-Tube Heat Exchanger using stable CuO/water nanofluid," Sustainable Energy Technologies and Assessments, vol. 31, no. December 2018, pp. 306-317, 2019, doi: 10.1016/j.seta.2018.12.020.
- [17] Sukarman et al., "Characterisation of TiO2 nanoparticles for nanomaterial applications: Crystallite size, microstrain and phase analysis using multiple techniques," *Nano-Structures & Nano-Objects*, vol. 38, 2024, doi: 10.1016/j.nanoso.2024.101168.
- [18] W. H. Azmi et al., "Experimental determination of turbulent forced convection heat transfer and friction factor with SiO2 nanofluid," *Experimental Thermal and Fluid Science*, vol. 51, pp. 103-111, 2013, doi: 10.1016/j.expthermflusci.2013.07.006.
- [19] M. Hojjat, "Nanofluids as coolant in a shell and tube heat exchanger: ANN modeling and multi-objective optimization," *Applied Mathematics and Computation*, vol. 365, pp. 124710-124710, 2020, doi: 10.1016/j.amc.2019.124710.
- [20] M. Setiyo et al., "Caractéristiques de l'effet refroidissant d'un système frigorifique à demicycle sur un système au GPL," *International Journal of Refrigeration*, vol. 82, pp. 227-237, 2017, doi: 10.1016/j.ijrefrig.2017.06.009.
- [21] I. M. Shahrul et al., "Effectiveness study of a shell and tube heat exchanger operated with nanofluids at different mass flow rates," Numerical Heat Transfer; Part A: Applications, vol. 65, no. 7, pp. 699-713, 2014, doi: 10.1080/10407782.2013.846196.
- [22] M. W. Tian et al., "Economic cost and efficiency analysis of the employment of inserting rods with helical fins in a shell and tube heat exchanger under magnetic field and filled with nanofluid," Ain Shams Engineering Journal, vol. 13, no. 4, pp.

- 101651-101651, 2022, doi: 10.1016/j.asej. 2021.11.020.
- [23] N. Tamilselvan, M. Thirumarimurugan, and E. Sudalai Manikandan, "Study on various control strategies of plate type heat exchanger for non-Newtonian fluids," *Journal of Ambient Intelligence and Humanized Computing*, vol. 12, no. 7, pp. 7253-7261, 2021, doi: 10.1007/s12652-020-02401-4.
- [24] D. Romahadi et al., "Bayesian networks approach on intelligent system design for the diagnosis of heat exchanger," *Sinergi*, vol. 26, no. 2, 2022, doi: 10.22441/sinergi.2022.2.001.
- [25] F. Anggara et al., "Numerical analysis of the vortex flow effect on the thermal-hydraulic performance of spray dryer," *Sinergi*, vol. 26, no. 1, 2022, doi: 10.22441/sinergi.2022.1.004.
- [26] R. Andrzejczyk and T. Muszyński, "Performance analyses of helical coil heat exchangers the effect of external coil surface modification on heat exchanger effectiveness," *Archives of Thermodynamics*, vol. 37, no. 4, pp. 137-159, 2016, doi: 10.1515/aoter-2016-0032.
- [27] M. H. Rostami et al., "Thermal performance investigation of SWCNT and graphene quantum dots nanofluids in a shell and tube heat exchanger by using fin blade tubes," *Heat Transfer,* vol. 49, no. 8, pp. 4783-4800, 2020, doi: 10.1002/htj.21852.
- [28] B. A. Saputra and N. Nurato, "Performance analysis of a single-cylinder type steam turbine with a capacity of 3.5 mw using enthalpy drop method," *Sinergi*, vol. 27, no. 3, 2023, doi: 10.22441/sinergi.2023.3.003.
- [29] S. P. Louis et al., "Application of Nanofluids in Improving the Performance of Double-Pipe Heat Exchangers—A Critical Review," *Materials*, vol. 15, no. 19, 2022, doi: 10.3390/ma15196879.
- [30] A. I. Ramadhan et al., "Experimental investigation on stability and thermal conductivity of SiO2 nanoparticles as green nanofluids for application thermal system," Sinergi, vol. 28, no. 3, 2024, doi: 10.22441/sinergi.2024.3.018.
- [31] E. M. Go et al., "Estimation of heat transfer coefficient of water and ethylene glycol mixture in nanopipe via non-equilibrium coarse-grained molecular dynamics," *Journal* of Industrial and Engineering Chemistry, vol. 77, pp. 128-134, 2019, doi: 10.1016/j.jiec.2019.04.027.
- [32] T. U. H. S. G. Manik, G. Sudrajat, and T. B. Sitorus, "The experimental study of the coolant flow rate of an ethylene glycol-mixed

- water to the heat transfer rate on the radiator," vol. 505, pp. 0-8. doi: 10.1088/1757-899X/505/1/012063
- [33] S. M. Abolarin, M. Everts, and J. P. Meyer, "Heat transfer and pressure drop characteristics of alternating clockwise and counter clockwise twisted tape inserts in the transitional flow regime," *International Journal of Heat and Mass Transfer,* vol. 133, pp. 203-217, 2019, doi: 10.1016/j.ijheatmasstransfer.2018.12.107.
- [34] A. Ghozatloo, M. Shariaty-Niasar, and A. M. Rashidi, "Investigation of Heat Transfer Coefficient of Ethylene Glycol/ Graphenenanofluid in Turbulent Flow Regime," *Int. J. Nanosci. Nanotechnol*, vol. 10, no. 4, pp. 237-244, 2014
- [35] N. Azari et al., "Experimental Investigation of Heat Transfer in Compact Heat Exchanger using Water-Ethylene Glycol," vol. 8, no. 04, pp. 666-669, 2019,
- [36] L. Karikalan, S. Baskar, N. Poyyamozhi, and Kassu Negash, "Experimental Analysis of Heat Transfer by Using Nanofluid and Impact of Thermophysical Properties," *Journal of Nanomaterials*, vol. 2022, 2022, doi: 10.1155/2022/5119797.
- [37] Dynalene TEG. "Dynalene TEG."
- [38] S. Tongfan and A. S. Teja, "Density, Viscosity, and Thermal Conductivity of Aqueous Ethylene, Diethylene, and Triethylene Glycol Mixtures between 290 K and 450 K," *Chemical Engineering Data,* vol. 48, pp. 198-202, 2003, doi: 10.1021/je025610o.
- [39] B. Kristiawan et al., "Thermo-hydraulic characteristics of anatase titania nanofluids flowing through a circular conduit," *Journal of Nanoscience and Nanotechnology*, vol. 16, no. 6, pp. 6078-6085, 2016, doi: 10.1166/jnn.2016.10902.
- [40] B. Kristiawan et al., "Enhancing the thermal performance of TiO2/water nanofluids flowing in a helical microfin tube," *Powder Technology*, vol. 376, pp. 254-262, 2020, doi: 10.1016/j.powtec.2020.08.020.
- Kumar and S. "Experimental study of Fe2O3/water and Fe2O3/ethylene glycol nanofluid transfer enhancement in a shell and tube heat exchanger." International Communications in Heat and Mass Transfer. vol pp. 277-284, 2016. 10.1016/j.icheatmasstransfer.2016.09.009.
- [42] A. Junaedi et al., "An Heat Transfer Coefficient and Pressure Characteristics in a Copper Pipe Flow System: A Preliminary study Utilizing an EG/Water Mixture," *Jurnal*

- *Teknik Mesin Mechanical Xplore*, vol. 4, no. 2, pp. 61-73, 2024, doi: 10.36805/jtmmx.v4i2.5920.
- [43] N. Arora and M. Gupta, "An experimental study on heat transfer and pressure drop analysis of Al2O3/water nanofluids in a circular tube," *Materials Today: Proceedings,* vol. 69, no. 2, pp. 199-204, 2022, doi: 10.1016/j.matpr.2022.08.347.
- [44] T. Thiyanaet al., "Heat Transfer Coefficient in a Copper Pipe Flow System Using a 40/60 Volume Ratio Ethylene Glycol/Water (EG/H2O) Blended Fluid," *Jurnal Teknik MesinMechanical Xplore (JTMMX)*, vol. 1, no. 2, pp. 37-46, 2023, doi: 10.36805/jtmmx.v4i1.5570.
- [45] A. Alimoradi, M. Olfati, and M. Maghareh, Numerical investigation of heat transfer intensification in shell and helically coiled finned tube heat exchangers and design optimization. Elsevier B.V., 2017, pp. 125-143.
- [46] M. R. Salem et al., "Effect of γ-Al2O3/water nanofluid on heat transfer and pressure drop characteristics of shell and coil heat exchanger with different coil curvatures," *Journal of Thermal Science and Engineering Applications*, vol. 7, no. 4, pp. 1-9, 2015, doi: 10.1115/1.4030635.
- [47] R. Barzegarian, A. Aloueyan, and T. Yousefi, "Thermal performance augmentation using water based Al2O3-gamma nanofluid in a horizontal shell and tube heat exchanger under forced circulation," *International Communications in Heat and Mass Transfer*, vol. 86, pp. 52-59, 2017, doi: 10.1016/j.icheatmasstransfer. 2017.05.021.
- [48] W. H. Azmi et al., "Heat transfer and friction factor of water based TiO2 and SiO2 nanofluids under turbulent flow in a tube," *International Communications in Heat and Mass Transfer*, vol. 59, pp. 30-38, 2014, doi: 10.1016/j.icheatmasstransfer.2014.10.007.
- [49] H. Chanson, "Applications of the Bernoulli equation to open channel flows," in Hydraulics of Open Channel Flow An Introduction Basic Principles, Sediment Motion, Hydraulic Modelling, Design of Hydraulic Structures, vol. 4: ELSEVIER, 2004. doi: https://doi.org/10.1016/B978-0-7506-5978-9.X5000-4
- [50] M. Sharifpur et al., "Optimum concentration of nanofluids for heat transfer enhancement under cavity flow natural convection with TiO2 – Water," *International Communications* in Heat and Mass Transfer, vol. 98, no. October, pp. 297-303, 2018, doi: 10.1016/j.icheatmasstransfer.2018.09.010.